

On Obtaining Reactive Potential Energy Surfaces from Transition State Photodetachment Spectra. I. Sensitivity Analysis

Ward H. Thompson[†]

Department of Chemistry, University of California, Berkeley, California 94720, and Department of Chemistry and Biochemistry, University of Colorado, Boulder, Colorado 80309-0215

Received: June 17, 1999; In Final Form: October 1, 1999

We investigate the possibility of obtaining potential energy surfaces for chemical reactions from experimental photodetachment spectra by carrying out a sensitivity analysis. Specifically, the variations of the theoretical photodetachment spectrum with respect to the values of the potential on a grid of points (the “derivatives” of the spectrum) are calculated. We show how these derivatives can be obtained at no extra cost beyond that required to obtain the spectrum. Sensitivity analysis is performed on one- and two-degrees-of-freedom model photodetachment systems. The results are discussed in the context of the prospects for the “inversion” of transition state spectra to obtain potential surfaces in reactive systems.

1. Introduction

For a chemical reaction, the barrier region is the most difficult part of the potential energy surface to obtain by electronic structure calculations, yet it is the most important in determining reactivity. A method for extracting this information from experimental measurements would thus be very useful. It is well established that transition state (photodetachment) spectroscopy experiments can directly probe the barrier region of a reactive potential energy surface.^{1–4} In these experiments a bound anion (e.g., ABC^-) is formed, the excess electron is detached by a photon of fixed energy to form the unstable neutral species (ABC^*), and the kinetic energy of the detached electron is measured. The resulting electron kinetic energy spectrum contains information about the reactive neutral potential energy surface (governing the $A + BC \rightarrow AB + C$ reaction). In particular, if the geometry of the anion is similar to that of the “activated complex” on the neutral surface, the spectrum contains detailed information about the neutral transition state. In this case, the spectrum will consist of peaks at the vibrational energy levels of the neutral activated complex (with intensities governed by the Franck–Condon overlap of the anion bound state and neutral scattering wave functions) with widths determined by the lifetimes of these states.

These experiments possess a number of advantages over conventional scattering experiments. For example, in reactive scattering experiments the measured cross sections include effects due to the entrance and exit valleys of the potential surface. However, the information about the barrier region contained in transition state spectra is not obscured in this way. Also, the information contained in the spectra is not averaged over many partial waves, which clouds the details of the reaction dynamics. This is actually a two-fold advantage as the corresponding theoretical calculations are more easily performed.

A straightforward method for obtaining a potential energy surface from a spectrum is a perturbative approach. That is, one calculates how the spectrum is affected (to first order) by changes in the neutral reactive potential, i.e., the “derivatives” of the spectrum. Given an experimental spectrum, these deriva-

tives can be used to obtain the potential surface giving the theoretical spectrum in best agreement with the experimental one. This can be accomplished by an iterative scheme in which, at each step, the potential is modified, using the derivatives, to minimize the “error” (i.e., the deviation of the theoretical spectrum from the experimental one) until convergence is reached. The following paper in this issue describes and applies such an approach.⁵

However, it is important to first understand what information is contained in transition state spectra before attempting to invert experimental spectra to obtain potential energy surfaces. Sensitivity analysis is a useful tool in determining an appropriate approach for inverting experimental spectra. For example, it can be used to decide if a “point-by-point” representation can be obtained from the spectra, if information about the barrier can be extracted when the Franck–Condon region does not overlap the transition state, and if spectra from vibrationally excited states of the anion can provide additional information. In this paper we address the question—To what part of the neutral potential energy surface are the photodetachment spectra sensitive? This question can be answered by examining the derivatives of the spectrum discussed above.

The theoretical approach for calculating photodetachment spectra and their derivatives with respect to potential parameters is described in Section 2. Particularly, we show how these derivatives can be obtained with no extra computational effort beyond that needed to calculate the photodetachment spectrum itself. To illustrate the basic features of the sensitivity of the photodetachment spectra to the neutral potentials, this method is implemented for two model transition state spectroscopy systems in Section 3. The results are discussed in terms of the prospects for inverting spectra to obtain potential energy surfaces. Finally, concluding remarks are given in Section 4.

2. Theory

In this section we review the theoretical methodology developed previously^{6,7} for efficiently calculating anion photodetachment intensities. We also show how this approach can be extended to calculate the derivatives of the photodetachment intensities with respect to parameters of the neutral potential surface with no extra computational cost.

[†] Current address. University of Colorado.

Consider a potential energy surface for a chemical reaction defined by a set of M parameters $\alpha = \{\alpha_j\}_{j=1,\dots,M}$. For example, the set α could be the values of the potential on a grid of points or the parameters in an analytical representation. The derivative $\partial I(E)/\partial\alpha_j$ indicates the first order dependence of the spectrum $I(E)$ on one of the parameters, α_j , and is thus a measure of the sensitivity of the spectrum to α_j . For example, if $\partial I(E)/\partial\alpha_j \approx 0$ then a small change in α_j will not change the spectrum. However, if $\partial I(E)/\partial\alpha_j$ has significant magnitude, varying α_j will modify the photodetachment intensity at energy E . Naturally, the derivative will depend on the value of α_j and the energy E at which this derivative is evaluated.

The photodetachment intensity is given within the Franck–Condon approximation as

$$I(E) = \rho(E) \sum_{\mathbf{n}} |\langle \Psi_{\mathbf{n}}^+(E) | \phi_b \rangle|^2, \quad (1)$$

where $\Psi_{\mathbf{n}}^+(E)$ is the scattering wave function on the neutral surface at energy E with outgoing wave boundary conditions and asymptotic quantum numbers \mathbf{n} , $\rho(E)$ is the neutral density of states, and ϕ_b is the bound state wavefunction of the anion. As shown previously,⁶ the photodetachment spectrum can be obtained using a discrete variable representation^{8–10} (DVR) Green's function with absorbing boundary conditions^{11–15} (ABC). In this formulation, the photodetachment intensity is given by⁶

$$I(E) = -\frac{1}{\pi} \text{Im} \phi_b^\top \cdot \mathbf{G}^+(E) \cdot \phi_b \quad (2)$$

where ϕ_b is the anion bound state wavefunction vector in the DVR basis and $\mathbf{G}^+(E)$ is the DVR-ABC Green's function,¹⁶

$$\mathbf{G}^+(E) = (E\mathbf{I} - \mathbf{H} + i\epsilon)^{-1} \quad (3)$$

with outgoing wave boundary conditions (as indicated by the superscript +). Here, $\mathbf{H} = \mathbf{T} + \mathbf{V}$ is the Hamiltonian matrix for the neutral species in the DVR basis and \mathbf{T} , \mathbf{V} , and ϵ are the kinetic energy, potential, and absorbing potential DVR matrices, respectively.

A prime advantage of this approach is that, in principle, the entire photodetachment spectrum can be obtained in a single calculation using the multiply shifted quasi-minimal residual (QMRES) method¹⁷ for acting the Green's function on the anion bound state.⁷ This is possible because the state upon which the Green's function is acted, ϕ_b , does not depend on the scattering energy. The reader is referred to ref 7 for a detailed description of this approach; here we concentrate only on the features relevant to the problem of calculating the sensitivity of photodetachment spectra.

In the expression for the photodetachment intensity in eq 2, the neutral potential energy surface appears only in the Green's function. Thus, taking the derivative of the photodetachment intensity with respect to a potential parameter α_j gives

$$\frac{\partial I(E)}{\partial\alpha_j} = -\frac{1}{\pi} \text{Im} \phi_b^\top \cdot \mathbf{G}^+(E) \cdot \frac{\partial \mathbf{V}}{\partial\alpha_j} \cdot \mathbf{G}^+(E) \cdot \phi_b \quad (4)$$

Note that, in the DVR, the potential operator, which is only a function of position, is approximated as a diagonal matrix with each diagonal element equal to the potential evaluated at the corresponding DVR grid point. If we define the scattering wavefunction,

$$\Phi_b^+(E) = \mathbf{G}^+(E) \cdot \phi_b \quad (5)$$

then

$$\Phi_b^+(E)^\top = \phi_b^\top \cdot \mathbf{G}^+(E) \quad (6)$$

(Note the absence of complex conjugation.) Then, eq 4 can be compactly written as

$$\frac{\partial I(E)}{\partial\alpha_j} = -\frac{1}{\pi} \text{Im} \Phi_b^{\top+}(E) \cdot \frac{\partial \mathbf{V}}{\partial\alpha_j} \cdot \Phi_b^+(E) \quad (7)$$

Analogous equations for this derivative have previously been derived in a time-dependent framework by Baer and Kosloff¹⁸ and in a time-independent formulation by Wu and Zhang.¹⁹ These workers have demonstrated their approaches by inverting absorption spectra (where the excitation is to a dissociative state).^{18,20}

The formulation of the derivative in terms of the DVR-ABC Green's function is new, however. Note that the major computational effort in calculating such a derivative via eq 7 is the same as that in obtaining $I(E)$: the action of the Green's function on the anion wavefunction. Thus, the derivative information can be generated with essentially no more effort than that required to calculate the photodetachment spectrum. In addition, this means that both the spectrum and all desired derivatives of the spectrum can be obtained at all energies in a single calculation using the QMRES method.

As an example, consider the potential as expressed in a discrete variable representation basis:

$$\hat{V} = \sum_{N_{\text{DVR}}}^{j=1} |j\rangle V_j \langle j| \quad (8)$$

Here, $|j\rangle$ is the j th DVR basis function localized about the grid point \mathbf{r}_j and V_j is the value of the potential at \mathbf{r}_j . The values of the potential at the DVR grid points can then be regarded as the parameters defining the potential. In this case, the derivatives have the particularly simple form

$$\frac{\partial I(E)}{\partial V_j} = -\frac{1}{\pi} \text{Im} [\Phi_b^+(E)]_j^2 \quad (9)$$

and thus reflect the form of the scattering wavefunction obtained from the action of the Green's function on the anion bound state. Equation 9 is the crucial formula for the purposes of this paper. In the following section, we use this equation to calculate these derivatives for two model systems to investigate the sensitivity of photodetachment spectra to the neutral potential energy surface.

3. Applications

A. Eckart Barrier. The one-dimensional Eckart barrier provides a simple, but quite useful, test problem for examining the basic properties of the sensitivity of the photodetachment spectrum to the neutral potential. In this model,²¹ the neutral potential is given by

$$V(q) = V_0 \text{sech}^2(q/a) \quad (10)$$

and the anion potential by

$$v_{\text{anion}}(q) = \frac{1}{2} m\omega^2 (q - q_0)^2 \quad (11)$$

In what follows, we take $V_0 = 0.425$ eV, $a = 1$ au, $m = 1060$ au, $\omega = 3000$ cm⁻¹, and different values of q_0 . The potentials

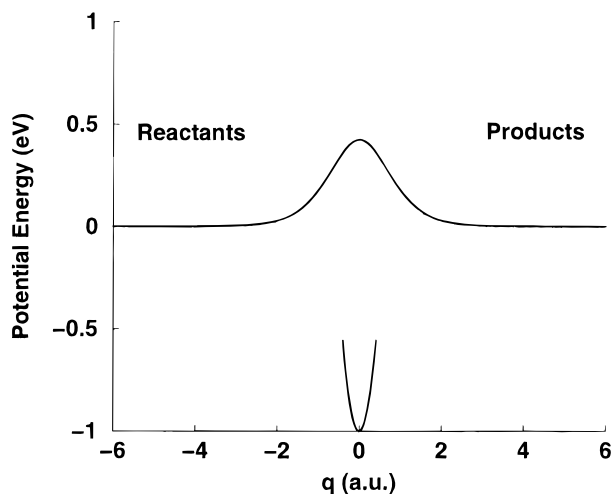


Figure 1. Depiction of the neutral and anion potential surfaces for the model one-dimensional Eckart barrier photodetachment system.

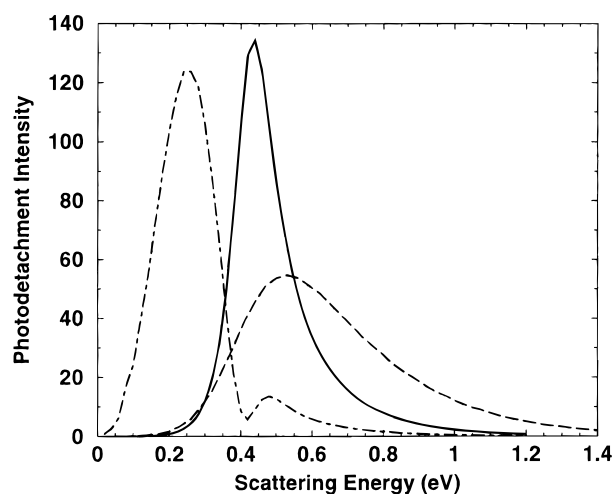


Figure 2. Photodetachment spectra for the one-dimensional model Eckart barrier system with $V_0 = 0.425$ eV, $a = 1$ au, $m = 1060$ au, and $\omega = 3000$ cm^{-1} . The photodetachment spectrum from the anion ground state ($\nu = 0$) with $q_0 = 0$ is shown as the solid line, the spectrum from the $\nu = 1$ anion state with $q_0 = 0$ as the dashed line, and the $\nu = 0$ spectrum with $q_0 = 1$ au as the dot-dashed line.

are shown in Figure 1 for $q_0 = 0$. For the purposes of discussion we define the reactants on the neutral surface as $q < 0$ and products as $q > 0$.

Figure 2 shows the photodetachment spectra calculated for the model Eckart barrier system in three different cases. The spectra are shown versus the scattering energy on the neutral surface for photodetachment from the $\nu = 0$ anion bound state with $q_0 = 0$, the $\nu = 1$ state with $q_0 = 0$, and the $\nu = 0$ state with $q_0 = 1$ au. The $\nu = 0, q_0 = 0$ spectrum consists of a single asymmetric peak centered around $E \approx 0.43$ eV $\approx V_0$. The anion wave function in this case is largest in the region of the barrier, leading to small intensities at energies below the barrier height where the neutral scattering wave function is decaying exponentially. The $\nu = 1, q_0 = 0$ spectrum has a similar structure but is peaked at ≈ 0.5 eV and has a tail at higher energies. Both differences reflect the better overlap of the $\nu = 1$ anion state with the more oscillatory neutral scattering wave functions at higher energies. The $\nu = 0, q_0 = 1$ au is peaked at ≈ 0.25 eV with a smaller peak around 0.48 eV. The displaced anion wave function is largest outside the barrier region leading to larger intensities at lower scattering energies.

Figure 3a shows the derivatives, at three different scattering

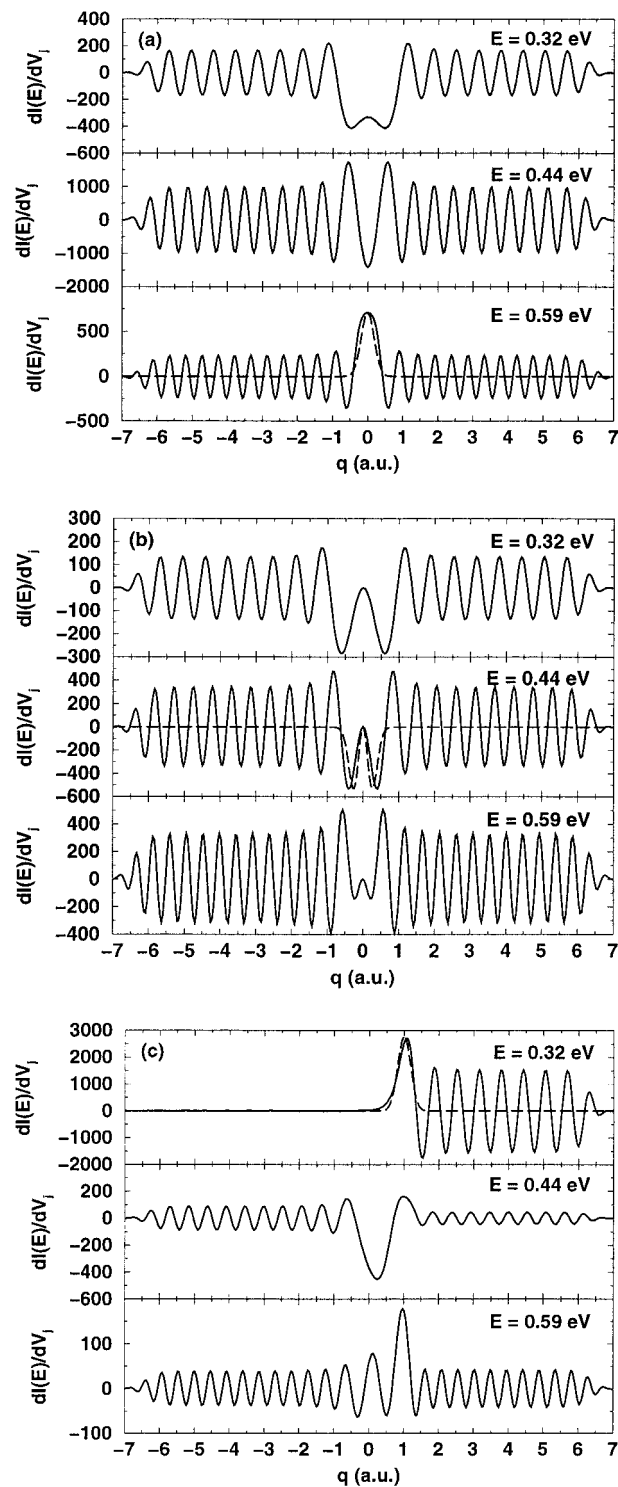


Figure 3. Sensitivity of the photodetachment spectrum to the neutral potential (in units of hartrees $^{-2}$) as represented on a DVR grid at three different values of the scattering energy. The absolute square of the anion wave function is indicated by a dotted line, scaled to be of the same magnitude as the sensitivity. Results are shown for (a) the $\nu = 0$ anion bound state with $q_0 = 0$, (b) the $\nu = 1$ anion bound state with $q_0 = 0$, and (c) the $\nu = 0$ anion bound state with $q_0 = 1$ au.

energies, of the photodetachment spectrum from the anion ground state with respect to the value of the neutral Eckart barrier potential at the DVR grid points, (cf. eq 8). Briefly, we use a sinc-function DVR basis¹⁰ to represent the Green's function and anion bound state. In this basis the DVR grid points are evenly spaced. For these calculations a significantly higher DVR grid density (Δq , the spacing between grid points ≈ 0.04

au) is used than is required to converge the photodetachment spectra in order to better observe the structure in the derivatives. The basic structure of the “sensitivity” is the same for all the energies. Namely, the derivatives of the spectrum with respect to the potential are (not surprisingly) largest in the Franck–Condon region and oscillate on both sides of this region.

It can be immediately seen that the frequency of these oscillations vary with the scattering energy. In fact, the wavelength of the oscillations at a given energy is precisely half the de Broglie wavelength corresponding to that scattering energy. That this should be so can be seen from eq 9, which shows that the derivative is proportional to the square of the scattering wave function. At large values of $|q|$, where the potential is flat, the scattering wavefunction has the form for $|q| \rightarrow \infty$

$$\Phi_b^+(E) \sim e^{ik|q|} \quad (12)$$

where $k = \sqrt{2mE}/\hbar$, so asymptotically

$$[\Phi_b^+(E)]^2 \sim e^{2ik|q|} \quad (13)$$

Thus, the presence of the square gives oscillations at a frequency twice that corresponding to the scattering energy. Note that the wave function decays to zero at the largest values of $|q|$ due to the absorbing boundary conditions.

The correspondence of the largest derivatives with the Franck–Condon region is particularly striking for energies significantly above the barrier. This can be seen in the bottom panel of Figure 3a ($E = 0.59$ eV) where the derivative of the spectrum with respect to the potential is superimposed with the absolute square of the anion wave function (suitably scaled).

This direct relationship is not observed for the two lower energies shown. The lowest energy, $E = 0.32$ eV, shown in the top panel of Figure 3a, is more than 0.1 eV below the barrier height and the magnitude of the derivative is peaked to either side of the barrier, where the anion bound state has greatest overlap with the scattering wave function at this energy. A similar pattern is observed for the derivative at $E = 0.44$ eV which is close to the barrier height. At this energy the derivative has positive peaks on either side of the center of the anion wave function and a negative peak at the center.

Figure 3b shows the derivatives of the photodetachment spectrum for the $\nu = 1$ anion bound state with $q_0 = 0$ with respect to the values of the neutral potential at the DVR grid points. There are some interesting differences between the structure seen here and that observed for the $\nu = 0$ ground state in Figure 3a. An important point to note is that for photodetachment from the $\nu = 1$ anion state the sensitivity is always zero at $q = 0$ (the center of the barrier) since the anion wave function has a node at that point.

The derivatives $\partial I(E)/\partial V_j$ at $E = 0.32$ eV are similar to that in Figure 3a for the $\nu = 0$ anion bound state. The primary difference is the node at $q = 0$ for the $\nu = 1$ spectrum. In both cases the spectrum is most sensitive to the sides of the neutral barrier. However, in the $\nu = 0$ case the derivative is nonzero near $q = 0$ due to the overlap between the exponentially decaying scattering wave function and the anion bound state which is largest in that region (cf. eq 1).

At all the energies, oscillations are again observed at a wavelength half of that corresponding to the scattering energy for large $|q|$. However, the $\nu = 1$ spectrum is somewhat more sensitive to the potential at larger values of $|q|$ than the $\nu = 0$ spectrum. This is not surprising since the $\nu = 1$ anion state is greater in extent than the ground state. However, it indicates

that additional information about the neutral potential, above that in the $\nu = 0$ spectrum, is contained in the spectra for vibrationally excited anion bound states.

The sensitivity of the photodetachment spectra from the $\nu = 0$ anion bound state with $q_0 = 1$ au in the anion potential, eq 11, is shown in Figure 3c for three different scattering energies. The case where the anion bound state does not sit directly under the neutral transition state is often the situation in realistic systems and is thus important to investigate.

The most striking difference between the $q_0 = 0$ (Figure 3a) and $q_0 = 1$ au sensitivities is at $E = 0.32$ eV where for $q_0 = 1$ au the derivative $\partial I(E)/\partial V_j$ is zero for $q < 0$. At this energy the transmission probability for the Eckart barrier is less than ~ 0.01 so photodetachment from this state yields only products.²¹ Thus, the spectrum is not sensitive to the reactant side of the potential.

At the scattering energy $E = 0.44$ eV the absolute value of the derivative peaks around $q \approx 0.24$ au and has significant magnitude in the barrier region. This is an important result as it indicates that information about the barrier may be obtained even when the Franck–Condon region for the photodetachment does not coincide with the transition state. The same is true for the sensitivity at $E = 0.59$ eV which consists of two large peaks and the usual oscillations at greater q . The dominant peak is at the position of the anion bound state, $q = 1$ au, while the smaller peak is centered at slightly positive values of q near $q = 0$. Thus, at this energy there is also sensitivity to the barrier region.

Recently, Skodje and co-workers²² have proposed a scheme for controlling the anion bound state in photodetachment systems. Their goal was to assign photodetachment spectra by changing the character of the anion state to accentuate, for example, resonance or direct scattering contributions. The large sensitivity of the spectrum to the neutral potential in the Franck–Condon region suggests that such a scheme could instead be used to map out the neutral potential energy surface.

B. Photodetachment of Collinear H_3^- . As a second application we consider a two-degrees-of-freedom model system in which the neutral potential energy surface is that for the collinear $\text{H} + \text{H}_2$ system²³ (as given by the LSTH surface²⁴). The anion potential is a separable harmonic oscillator potential in the Jacobi coordinates of the reactant arrangement:

$$v_{\text{anion}}(r, R) = \frac{1}{2}\mu_r\omega_r^2(r - r_0)^2 + \frac{1}{2}\mu_R\omega_R^2(R - R_0)^2. \quad (14)$$

Here, r is the diatomic H_2 distance in the reactants and R is the distance from the center of mass of H_2 to the colliding H atom; μ_r and μ_R are the reduced masses associated with these coordinates and ω_r and ω_R are the harmonic frequencies of the anion potential in these coordinates. The classical barrier to reaction is 0.425 eV for the LSTH surface.

We examine two different parameter sets for the anion potential which we will refer to as Sets A and B. In Set A the anion equilibrium geometry lies directly under the neutral transition state with $\omega_r = 2500$ cm^{-1} , $r_0 = 1.757$ au, $\omega_R = 2000$ cm^{-1} , and $R_0 = 2.6355$ au. The frequencies are kept the same but the anion equilibrium geometry is displaced into the reactant valley in parameter Set B for which $r_0 = 1.6$ au and $R_0 = 3.2$ au

The photodetachment spectra for this model collinear H_3^- photodetachment system are shown in Figure 4 for the two parameter sets. Figure 5 shows a contour plot of the neutral $\text{H} + \text{H}_2$ (LSTH) potential superimposed with the anion bound states for parameter Sets A and B. The spectrum with parameter Set A is peaked around a scattering energy of $E \approx 0.56$ eV,

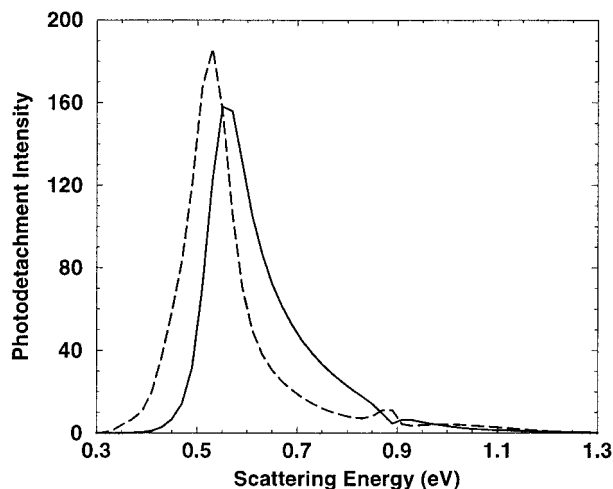


Figure 4. Photodetachment spectra for the model collinear H_3^- system. The spectrum obtained using parameter Set A for the anion potential is given by the solid line, while the spectrum for Set B is shown as the dashed line.

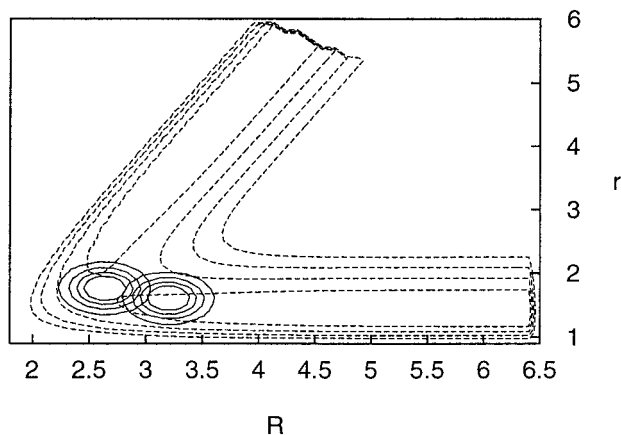


Figure 5. Contour plot of the LSTH potential energy surface and the absolute square of the anion bound state wave functions for the model collinear H_3^- photodetachment model system. The wave function for the anion potential parameter Set A appears to the left of that for Set B. The contours for the potential surface are spaced 0.4 eV apart from 0.4 to 2.4 eV; for the wave functions the contours range from 0.008 to 0.032 in increments of 0.008. The distances R and r are in atomic units.

corresponding to the threshold for reaction in the collinear $\text{H} + \text{H}_2$ system. In analogy with the Eckart barrier model considered above, the displaced anion potential of parameter Set B leads to a spectrum peaking at somewhat lower energies. Both spectra have structure around $E = 0.9$ eV relating to the threshold for production of H_2 ($\nu = 1$). The threshold for reaction into (or out of) the $\nu = 1$ state of H_2 for collinear $\text{H} + \text{H}_2$ occurs at ~ 0.88 eV.²⁵

Figure 6 shows some illustrative examples of the sensitivity of the photodetachment spectra to the neutral potential for the model H_3^- system. Many of the general features of the sensitivities in this system are the same as in the one-dimensional Eckart barrier model considered above. Specifically, the magnitude of the derivative, $\partial I(E)/\partial V_j$, peaks in the vicinity of the Franck–Condon region and the derivative exhibits oscillatory structure in the reactant and product asymptotic valleys with a wavelength dependent on the scattering energy. However, there are some noteworthy differences as well as further similarities which we now discuss.

In Figure 6a contour plots of the derivative $\partial I(E)/\partial V_j$ and the neutral potential are shown for parameter Set A at a scattering

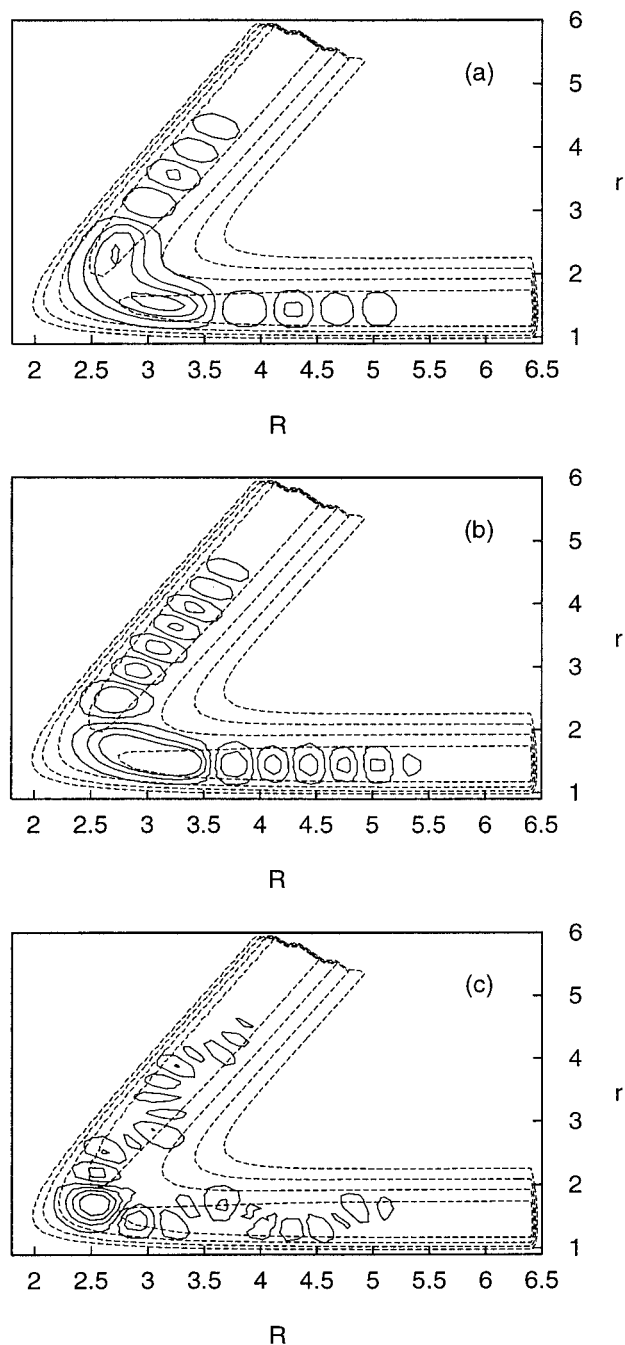


Figure 6. The sensitivity of the photodetachment spectrum for the collinear H_3^- model system is shown. (a) Results using anion potential parameter Set A and a scattering energy of $E = 0.49$ eV; the contours for the sensitivity range from -600 to 100 in increments of 175 in units of hartrees⁻². (b) Results using anion potential parameter Set B and a scattering energy of $E = 0.59$ eV; the contours for the sensitivity range from -350 to 650 in increments of 250 in units of hartrees⁻². (c) Results using anion potential parameter Set A and a scattering energy of $E = 0.95$ eV; the contours for the sensitivity range from -40 to 85 in increments of 25 in units of hartrees⁻². The distances R and r are in atomic units.

energy of $E = 0.49$ eV. The sensitivity has a large negative doubly peaked maximum encompassing much of the transition state region and extending significantly into the reactant and product valleys. This energy is below the threshold for reaction in the collinear $\text{H} + \text{H}_2$ system and reaction occurs only through tunneling. Thus, as observed for the Eckart barrier model (cf. $E = 0.32$ eV in Figure 3a), the spectrum at this energy is most sensitive to the sides of the barrier. A more subtle detail of this

plot is that the magnitude of the sensitivity is largest somewhat away from the transition state where the anion bound state is largest. In fact, the sensitivity here is somewhat suggestive of the "corner-cutting" nature of tunneling.²⁶

An analogous contour plot is shown in Figure 6b but for parameter Set B and at a scattering energy of $E = 0.59$ eV. In this case the sensitivity peaks in a broad area extending from the Franck–Condon region (recall that here the anion bound state is displaced toward the reactant valley) to the transition state. This is a very interesting result in that it shows that for this system the photodetachment spectrum is sensitive to the barrier region even when the anion wave function is small or zero there. This is encouraging from the point of view of using spectra to obtain information about potential surfaces, particularly in the transition state region.

Figure 6c shows the derivative $\partial I(E)/\partial V_j$ and the neutral potential for parameter Set A at a scattering energy of $E = 0.95$ eV. The most striking feature of the sensitivity at this energy is the nodal structure in the vibrational H_2 coordinate in the asymptotic valleys. This is present because photodetachment is now leading to the production of H_2 ($\nu = 1$) in both the reactants and products. Another interesting difference from Figure 6, parts a and b, is that the derivative is largest near the repulsive wall occurring for smaller values of H–H distances in the transition state.

4. Concluding Remarks

We have shown how the derivatives of photodetachment intensities with respect to parameters of the neutral potential energy surface can be calculated within the DVR-ABC Green's function formulation. These derivatives can be obtained with no extra computational effort beyond that required to calculate the photodetachment spectrum itself. In addition, using the quasi-minimal residual method for applying the Green's function onto the anion bound state, both the spectrum and any desired derivatives can be obtained at all energies in a single calculation.

We have examined the sensitivity of the photodetachment spectra to the neutral potential energy surfaces for two model systems to illustrate the general features in transition state spectroscopy systems. In general, the spectrum is most sensitive to the neutral potential in the Franck–Condon region where the anion wave function is largest and in the area around the transition state. The spectra do not appear to be sensitive to the global potential surface. This is discouraging from the point of view of inverting a transition state spectrum to obtain the potential in a "point-by-point" representation. However, the results are quite encouraging if the goal is extracting information about the potential in the region of the barrier. This is, after all, the most difficult part of the potential to obtain by other means, e.g., ab initio calculations.

Acknowledgment. I gratefully acknowledge Prof. William H. Miller for his generous support and encouragement as well as for many productive conversations and Prof. James T. Hynes for his support during the completion of this work. I also thank Prof. Daniel M. Neumark for useful discussions.

References and Notes

- (1) Neumark, D. M. *Acc. Chem. Res.* **1993**, *26*, 33; Metz, R. B.; Bradforth, S. E.; Neumark, D. M. *Adv. Chem. Phys.* **1992**, *81*, 1.
- (2) Weaver, A.; Metz, R. B.; Bradforth, S. E.; Neumark, D. M. *J. Chem. Phys.* **1990**, *93*, 5352; Weaver, A.; Neumark, D. M. *Faraday Discuss. Chem. Soc.* **1991**, *91*, 5; Bradforth, S. E.; Arnold, D. W.; Neumark, D. M.; Manolopoulos, D. E. *J. Chem. Phys.* **1993**, *99*, 6345.
- (3) Manolopoulos, D. E.; Stark, K.; Werner, H. J.; Arnold, D. W.; Bradforth, S. E.; Neumark, D. M. *Science* **1993**, *262*, 1852.
- (4) Schatz, G. C. *J. Chem. Phys.* **1989**, *90*, 3582; Schatz, G. C. *J. Chem. Phys.* **1989**, *90*, 4847; Schatz, G. C. *J. Phys. Chem.* **1990**, *94*, 6157.
- (5) Thompson, W. H. *J. Phys. Chem. A* **1999**, *103*, 9506.
- (6) Thompson, W. H.; Miller, W. H. *J. Chem. Phys.* **1994**, *101*, 8620.
- (7) Thompson, W. H.; Karlsson, H. O.; Miller, W. H. *J. Chem. Phys.* **1996**, *105*, 5387.
- (8) Dickinson, A. S.; Certain, P. R. *J. Chem. Phys.* **1963**, *49*, 4209; Harris, D. O.; Engerholm, G. G.; Gwinn, W. D. *J. Chem. Phys.* **1965**, *43*, 1515.
- (9) Lill, J. V.; Parker, G. A.; Light, J. C. *Chem. Phys. Lett.* **1982**, *89*, 483; Light, J. C.; Hamilton, I. P.; Lill, J. V. *J. Chem. Phys.* **1985**, *82*, 1400; Bačić, Z.; Light, J. C. *J. Chem. Phys.* **1986**, *85*, 4594; Whitnell, R. M.; Light, J. C. *J. Chem. Phys.* **1988**, *89*, 3674; Choi, S. E.; Light, J. C. *J. Chem. Phys.* **1990**, *92*, 2129.
- (10) Colbert, D. T.; Miller, W. H. *J. Chem. Phys.* **1992**, *96*, 1982.
- (11) Goldberg, A.; Shore, B. W. *J. Phys. B* **1978**, *11*, 3339.
- (12) Leforestier, C.; Wyatt, R. E. *J. Chem. Phys.* **1983**, *78*, 2334.
- (13) Jolicard, G.; Austin, E. J. *Chem. Phys. Lett.* **1985**, *121*, 106; Jolicard, G.; Austin, E. J. *Chem. Phys.* **1986**, *103*, 295; Jolicard, G.; Perrin, M. Y. *Chem. Phys.* **1987**, *116*, 1; Jolicard, G.; Leforestier, C.; Austin, E. J. *J. Chem. Phys.* **1988**, *88*, 1026.
- (14) Kosloff, R.; Kosloff, D. *J. Comput. Phys.* **1986**, *63*, 363.
- (15) Neuhauser, D.; Baer, M. *J. Chem. Phys.* **1989**, *90*, 4351; Neuhauser, D.; Baer, M. *J. Chem. Phys.* **1989**, *91*, 4651; Neuhauser, D.; Baer, M.; Kouri, D. J. *J. Chem. Phys.* **1990**, *93*, 2499.
- (16) Seideman, T.; Miller, W. H. *J. Chem. Phys.* **1992**, *96*, 4412; Seideman, T.; Miller, W. H. *J. Chem. Phys.* **1992**, *97*, 2499; Miller, W. H.; Seideman, T. In *Time Dependent Quantum Molecular Dynamics: Experiment and Theory*; Broeckhove, J., Ed.; NATO ARW 1992; Thompson, W. H.; Miller, W. H. *Chem. Phys. Lett.* **1993**, *206*, 123.
- (17) Freund, R. W.; Nachtigal, N. M. *Numer. Math.* **1991**, *60*, 315; Freund, R. W. In *Numerical Linear Algebra*; Reichel, L., Ruttan, A., Varga, R., Eds.; de Gruyter: Berlin, 1993.
- (18) Baer, R.; Kosloff, R. *Chem. Phys. Lett.* **1992**, *200*, 183.
- (19) Wu, Q.; Zhang, J. Z. H. *Spectrochim. Acta A* **1997**, *53*, 1189.
- (20) Wang, D.; Zhang, J. Z. H. *J. Chem. Phys.* **1998**, *108*, 10027.
- (21) Thompson, W. H. Ph.D. Thesis, Lawrence Berkeley Laboratory, University of California, 1996.
- (22) Sadeghi, R.; Skodje, R. T. *J. Chem. Phys.* **1996**, *105*, 7504; Skodje, R. T.; Sadeghi, R.; Krause, J. L. *Trans. Faraday Soc.* **1997**, *93*, 765; Skodje, R. T.; Sadeghi, R.; Krause, J. L. *Chem. Phys.* **1999**, *240*, 129.
- (23) Spath, B. W.; Miller, W. H. *Chem. Phys. Lett.* **1996**, *262*, 486.
- (24) Liu, B.; Siegbahn, P. *J. Chem. Phys.* **1978**, *68*, 2457; Truhlar, D. G.; Horowitz, C. *J. Chem. Phys.* **1978**, *68*, 2566; *J. Chem. Phys.* **1979**, *71*, 1514.
- (25) Bondi, D. K.; Connor, J. N. L. *J. Chem. Phys.* **1985**, *82*, 4383.
- (26) See, for example, George, T. F.; Miller, W. H. *J. Chem. Phys.* **1972**, *56*, 5722.